Author's Accepted Manuscript

Amperometric bioaffinity sensing platform for avian influenza virus proteins with aptamer modified gold nanoparticles on carbon chips

Farhana Sharmin Diba, Suhee Kim, Hye Jin Lee

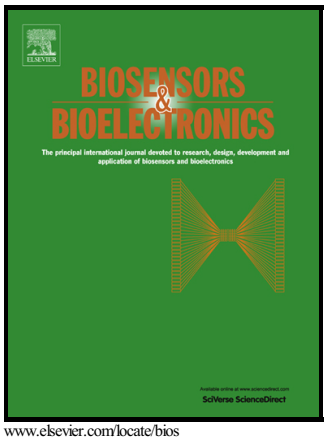

www.elsevier.com/locate/bios

PII: S0956-5663(15)30116-0
DOI: http://dx.doi.org/10.1016/j.bios.2015.05.020
Reference: BIOS7682

To appear in: *Biosensors and Bioelectronic*

Received date: 16 March 2015
Revised date: 5 May 2015
Accepted date: 7 May 2015

Cite this article as: Farhana Sharmin Diba, Suhee Kim and Hye Jin Lee, Amperometric bioaffinity sensing platform for avian influenza virus proteins with aptamer modified gold nanoparticles on carbon chips, *Biosensors and Bioelectronic,* http://dx.doi.org/10.1016/j.bios.2015.05.020

This is a PDF file of an unedited manuscript that has been accepted for publication. As a service to our customers we are providing this early version of the manuscript. The manuscript will undergo copyediting, typesetting, and review of the resulting galley proof before it is published in its final citable form. Please note that during the production process errors may be discovered which could affect the content, and all legal disclaimers that apply to the journal pertain.

ACCEPTED MANUSCRIPT

Amperometric bioaffinity sensing platform for avian influenza virus proteins with aptamer modified gold nanoparticles on carbon chips

Farhana Sharmin Diba, Suhee Kim and Hye Jin Lee*

Department of Chemistry and Green-Nano Materials Research Center, Kyungpook National University, 80 Daehakro, Buk-gu, Daegu-city, 702-701, Republic of Korea

*E-mail address: hyejinlee@knu.ac.kr and Phone number: +82 (053) 950-5336

Abstract:

A sandwich assay platform involving a surface formed aptamer-protein-antibody complex was developed to obtain the highly selective and sensitive amperometric detection of H5N1 viral proteins using a gold nanoparticle (NP) modified electrode. This is the first aptamer-antibody pairing reported for the selective detection of H5N1. Nanoparticle deposited screen-printed carbon electrodes were first functionalized by the covalent immobilization of a DNA aptamer specific to H5N1 followed by the adsorption of H5N1 protein. Alkaline phosphatase (ALP) conjugated monoclonal antibody was then adsorbed to form a surface bound Au NPs-aptamer/H5N1/antiH5N1-ALP sandwich complex which was further reacted with the enzyme substrate, 4-amino phenyl phosphate (APP). The current associated with the electrocatalytic reaction of the surface bound ALP with APP increased as the H5N1 concentration increased. A lowest detectable concentration of 100 fM was obtained with a linear dynamic range of 100 fM to 10 pM using differential pulse voltammetry. As an example, the biosensor was applied to the detection of H5N1 protein in diluted human serum samples spiked with different concentrations of the viral protein target.

Key words : Surface sandwich assay; H5N1 detection; Biofunctionalized electrode; DNA aptamer; Electrochemical detection; Au nanoparticle deposition

Accepted manuscript

1. Introduction

ACCEPTED MANUSCRIPT

Over the last decade highly pathogenic avian influenza virus of type A of subtype, H5N1, have resulted in 668 cases of human infection (WHO, 2014) in addition to a loss of over $760 million worldwide in the poultry industry (Burns et al., 2008). Adverse effects of H5N1 on economic as well as social wellbeing necessitates the need for a rapid, field applicable, sensitive and reliable method to detect H5N1 as a precautionary step to control the spread and for diagnostic purposes (Kamikawa et al., 2010; Wei et al., 2013). Typically employed methods to detect H5N1 include serological tests (Desvaux et al., 2012), enzyme-linked immunosorbent assays (ELISAs) (He et al., 2010; Zhu et al., 2014; Lebarbenchon et al., 2012; Moreno et al., 2013), immunoblotting (Jackson et al., 2010), reverse transcription polymerase chain reaction (Dhumpa et al., 2011) and western blot assay (Uyeki et al., 2012). But these methods are associated with some disadvantages like requiring excessive reagents, long sensing time, complicated sample processing and further sophisticated tests for confirmation leading to an urge to develop a portable and robust biosensor (Kamikawa et al., 2010; Wei et al., 2013). High levels of sensitivity, cost effective fabrication and easy handling in addition to low sample quantity requirement make electrochemical biosensors one of the outstanding candidates (Lv et al., 2010 ; Ricci et al., 2012; Ionescu et al., 2007).

Accepted manuscript

ACCEPTED MANUSCRIPT

Considerable research has also been undertaken on creating a diverse range of optical and electrochemical H5N1 sensors over the past few years. For example, fluorescence biosensors based on metal organic frameworks with a detection limit of 1.6 nM (Wei et al., 2013), and a CdTe quantum dot based biosensor with a detection limit of 3 $ng\,mL^{-1}$ (Nguyen et al., 2012). QCM aptasensors and magnetic nanobeads amplified QCM immunosensors were also been reported for the detection of H5N1 protein (Brockman et al., 2013; Li et al., 2011). Alternatively, electrochemical biosensors have also been reported as a promising approach; for instance, the label-free detection of H5N1 protein using indium-tin-oxide thin film transistors showed a detection limit of 80 $pg\,mL^{-1}$ (Guo et al., 2013), while a carbon nanotube network field effect transistor was reported to detect 1.25 pM H5N1 protein (Thu et al., 2013). In addition, non-faradic impedance biosensors and microelectrode based impedance immunosensors have been proved as a potential method for H5N1 hemagglutinin (Lum et al., 2012; Wang et al., 2009). Another method based on immobilization of polydiacetylene vesicles on to a polystyrene microsphere surface was also investigated and a detection limit of 1 $ng\,mL^{-1}$ for H5N1 protein was achieved using both electrochemical and fluorescence measurements (Dong et al., 2013).

Accepted manuscript

The integration of nanomaterials within electrochemical sensors can provide greater flexibility, functionalities and controlled properties within various detection format (Hayat et al., 2014). For example, the detection of H5N1 gene sequence has been reported based on electrically active magnetic nanoparticles and glassy carbon electrodes modified with carbon nanotubes-cobalt phthalocyanine-polyamidoamine dendrimer nanocomposites (Kamikawa et al., 2010; Zhu et al., 2009) achieving a detection limit of 1.4 μM and 1.0 pg mL^{-1}, respectively. In particular, Au NPs have been widely employed for developing biosensors due to their exceptional electrochemical properties, excellent catalytic behavior and providing a greater active surface area and biocompatibility such as for enzyme immobilization (Pingarron et al., 2008). We have also reported the combined use of Au NPs and surface enzyme reactions to enhance the sensitivity and selectivity of electrochemical biosensors for immunoglobulin E, phenol and catechol (Nam et al., 2012; Karim and Lee, 2013; Karim et al., 2014).

In this paper, we demonstrate a novel, portable and highly reproducible amperometric biosensing platform composed of a surface sandwich complex of H5N1 aptamer/H5N1 protein/H5N1 antibody conjugated with alkaline phosphatase (antiH5N1-ALP) formed on a gold nanoparticle modified screen printed carbon electrode (SPCE). The advantages of using aptamers when available instead of antibodies is well established (e.g. chemical

ACCEPTED MANUSCRIPT

stability and synthesis, reproducibility, selectivity) (Cho et al., 2009; Lee et al., 2008). We have also shown aptamer-functionalized surfaces to be superior to antibodies for bioaffinity measurements in serum both in terms of non-specific interactions and higher specificity (Jang et al., 2014). The H5N1 specific aptamer-antibody pairing introduced in this work is being reported for the first time with the electrochemical detection signal enzymatically amplified utilizing ALP to create an electroactive substrate in the presence of the protein target. Recently, Liu et al reported the electrochemical detection of a synthetic H5N1 gene sequence via a redox active DNA intercalator using a hybrid electrode composed of Au NPs, polypyrrole nanowires and carbon nanotubes assembled on a gold surface (Liu et al., 2011). Our measurements were performed on a screen-printed carbon electrode (SPCE) onto which Au nanoparticles (NP's) were electrochemically deposited followed by surface functionalization. Following validation of the aptamer-antibody pairing, the electrocatalytic reaction of the surface bound ALP with APP substrate was correlated to H5N1 concentration via both cyclic (CV) and differential pulse (DPV) voltammetries. In addition, the biosensors were employed for the analysis of H5N1 concentrations spiked into diluted serum samples.

2. Experimental Section

ACCEPTED MANUSCRIPT

2.1. Reagents and solutions

All of the chemicals listed here were used as received unless otherwise specified. Gold (III) chloride trihydrate ($HAuCl_4$, Sigma-Aldrich), N-(3-dimethylaminopropyl)-N'-ethylcarbodiimide hydrochloride (EDC, Thermo), 3-mercaptopropionic acid (MPA, Sigma-Aldrich), 11-mercaptoundecanoic acid (MUA, Sigma-Aldrich), N-hydroxysulfosuccinimide (NHSS, Thermo), sulfuric acid, 95%, (OCI Company Ltd), tris(hydroxymethyl)-aminomethane (≥99.9%, Sigma-Aldrich), potassium chloride (Merck), magnesium chloride anhydrous (Junsei Chemical Co., Ltd), 4-aminophenylphosphate monosodium salt (APP, LKT Laboratories, Inc.), influenza A virus hemagglutinin H5 full length protein (Abcam), human serum from human male AB plasma (Sigma-Aldrich), minisart SRP 4 syringe filter (pore size = 0.2 µm, Sartorius Stedim Biotech GmbH), influenza A virus hemagglutinin H5 monoclonal antibody (Abnova), H5N1 DNA aptamer sequence: 5'- TTG GGG TTA TTT TGG GAG GGC GGG GGT T-NH_2-3' (Shiratori et al., 2014) and NC4 control sequence: 5'-H_2N-GGG GCA CGT ACG GGC ATC ATA ACA ACA GGC GTG CCC C-3' were synthesized by Integrated DNA Technologies (IDT). Also, immunoglobulin G from human serum (IgG, Sigma-Aldrich), albumin from human serum lyophilized powder (globulin free, Sigma-Aldrich), brain natriuretic peptide (BNP, Tocris) and alpha-1 antitrypsin antibody (antiAAT, R&D Systems), were used along with the NC4 sequence for non-specific

ACCEPTED MANUSCRIPT

interaction and selectivity studies. 10 mM phosphate buffered saline (PBS, pH 7.4, Gibco) was used as a storage buffer for H5N1 protein, H5N1-aptamer and antiH5N1. AntiH5N1 was conjugated with ALP using a ALP labeling kit-NH_2 (Dojindo Molecular Technologies, Inc.) following the protocol provided by the company website (www.dojindo.com/store/p/47-Alkaline-Phosphatase-Labeling-Kit-NH2.html). The electrocatalytic reaction between ALP and APP was performed in 50 mM Tris buffer solution containing 10 mM KCl and 1 g/L of $MgCl_2$ (pH 8.5) at room temperature (Nam et al., 2012). Millipore-filtered water was used to make all aqueous solutions.

Accepted manus

2.2. Validation of aptamer-antibody pairing

A series of SPR measurements were performed to verify the antibody and aptamer bioaffinity interactions both separately and in a sandwich assay format. These measurements were also used to confirm surface activity on a gold surface and obtain binding coefficients for each probe. A Biacore 3000 at the National Nanofab Center (Daejeon) was used at a flow rate of 5 μL/min and a running buffer of PBS (pH 7.4) solution was used throughout. Further experimental details on the gold film SPR chips and data acquisition are provided in the supporting information.

2.3. Electrochemical measurements

ACCEPTED MANUSCRIPT

All electrochemical investigations were performed using a computer controlled potentiostat (Autolab PGSTAT128N, Ecochemie) operated by General Purpose Electrochemical System (GPES) version 4.9 software package. Screen printed carbon electrodes (SPCE) consisting of a carbon working electrode with a geometric area of a 28 mm^2, a Ag/AgCl reference electrode and a carbon counter electrode were purchased from The BIO Co., Ltd. SPCE's were connected with the potentiostat using a sensor connector. CV and DPV were used throughout the experiments with the condition as follows: for CV, the scan rate of 50 mV/s, while for DPV, the step potential of 20 mV/s, pulse interval of 50 ms and amplitude of 50 mV.

2.4. Electrodeposition of gold nanoparticles on SPCE

Electrodeposition of Au NPs was performed onto carbon working electrodes using a well-established method that has been previously reported (Karim and Lee, 2013; Renedo and Martínez, 2007; Barquero-Quirós et al., 2014; Alvarado-Gámez et al., 2015; Alonso-Lomillo et al., 2009). SPCEs were immersed into a 0.5 M H_2SO_4 solution containing 0.5 mM $HAuCl_4$ followed by applying a constant potential of 0.18 V (vs. Ag/AgCl) for 400 s while stirring. The Au NP deposited SPCE was then thoroughly washed with water and dried using a N_2 stream.

Accepted manuscript

ACCEPTED MANUSCRIPT

2.5. Biofunctionalization of gold deposited electrode surface

Au NP deposited SPCEs were soaked in 20 mM MPA solution prepared in absolute ethanol/water in a v/v ratio of 75/25 for 15 h at room temperature leading to the formation of a self-assembled carboxylic acid terminated monolayer. The bulk concentrations and timescales used for MPA coating of the electrodeposited Au NP's are sufficient to ensure that a maximum steady-state surface coverage is obtained, which has been estimated in the literature at about 70-80% (Limbut et al., 2006). Subsequently, the electrodes were rinsed with ethanol and water to remove excess MPA and dried under a N_2 stream. A 50 µL mixed solution of 75 mM EDC and 15 mM NHSS in 10 mM PBS (pH 7.4) was then drop casted on the MPA modified Au NPs coated electrodes for 30 min followed by rinsing with water and drying. About 80% of MPA will be activated by the EDC/NHSS along with biocompatibility (Limbut et al., 2006; Wang et al., 2011). Next, a 1 µL aliquot of 10 nM H5N1 aptamer was spread over the chip surface by covering with a piranha treated glass cover slip for 3 h. Following aptamer immobilization, the chips were then washed with 10 mM PBS (pH 7.4) and ready to use.

2.6. Electrochemical reactions for H5N1 detection

A 1 µL aliquot of different concentrations of H5N1 protein was drop casted and spread on the aptamer functionalized chip and incubated for at least 1 h. After washing the chip

Accepted manuscript

with 10 mM PBS (pH 7.4), 1 µL of 50 nM antiH5N1-ALP was drop casted and spread on the H5N1/aptamer surface and incubated for a minimum 1 h followed by rinsing with 50 mM Tris buffer (pH 8.5). This results in the formation of Au NP-H5N1-aptamer/H5N1/antiH5N1–ALP surface sandwich complexes which was assembled in an electrochemical cell containing a total volume of 5 mL of 50 mM Tris buffer, 10 mM KCl and 1 g/L of $MgCl_2$ (pH 8.5). A 30 µL aliquot of 10 mM APP was then added to the cell (final concentration = 60 µM). The electrocatalytic reaction of surface bound ALP sandwich complex with APP was monitored using CV and DPV. When investigating non-specific interactions, BNP and antiAAT-ALP were used instead of H5N1 and antiH5N1, respectively. Also the NC4 control aptamer was used instead of the H5N1 aptamer. For serum analysis, the serum sample was filtered using a Minisart SRP 4 syringe filter prior to use and diluted in 10 mM PBS buffer (pH 7.4).

Accepted manuscript

3. Results and Discussion

3.1. Detection methodology for H5N1

A schematic of the aptamer-antibody sandwich assay platform for H5N1 detection on a Au NP modified screen printed carbon electrode (SPCE) is depicted in Figure 1. Gold nanoparticles were first electrodeposited onto the SPCE and then subsequently functionalized with carboxylic acid terminated monolayer to enable the covalent

attachment of a 5'-amine modified H5N1 DNA aptamer. The sequential adsorption of H5N1 protein and antiH5N1-ALP conjugate onto the DNA aptamer results in the formation of a surface aptamer/protein/antibody-ALP complex. The electrocatalytic reaction of the surface bound ALP with 4-aminophenyl phosphate (APP) substrate was then used for the quantitative analysis of H5N1. The combined use of both an antibody and an aptamer bioreceptor specific to H5N1 protein was designed to improve selectivity and also further enhance measurement sensitivity.

3.2 Validation of aptamer-antibody pairing

Prior to performing electrochemical detection, a series of measurements were performed using surface plasmon resonance (SPR) to first confirm that both the aptamer and antibody simultaneously bind to different epitope sties on the H5N1 protein. A similar probe attachment chemistry was applied on the SPR chip surface to that of the electrochemical sensor (see supporting info for more details). Next, a series of measurements were performed where both aptamer and antiH5N1 functionalized chips were exposed to a range of H5N1 target concentrations and the resulting SPR signal normalized with respect to a negative control signal. The Langmuir adsorption isotherm plots derived from this data are shown in figure 2(a) and (b) with analysis revealing strong surface binding affinities of K_{ads} = 2.09 (±0.01) x 10^7 M^{-1} and 1.17 (±0.01) x 10^8

Accepted manuscript

M^{-1} for the antiH5N1 and DNA aptamer modified gold chips, respectively. The strong interaction between H5N1 and antiH5N1 is in good agreement with that reported previously (Hu et al., 2012) while this is the first time that a value for the interaction between the aptamer and H5N1 has been reported. Due to the aptamer having a higher affinity towards the target protein compared to antiH5N1 and the commercial availability of kits for ALP conjugation to an antibody, an aptamer-modified surface was preferred for creating the sandwich assay.

To then confirm that both the aptamer and antibody probes can be used simultaneously, the data in figure 2(c) shows results where a 200 nM H5N1 target solution was first exposed to an aptamer modified chip resulting in a high fractional surface coverage (θ). When different concentrations of antiH5N1 were next introduced to the chip, the normalized SPR signal (obtained by subtracting control channels either exposed to 200 nM thrombin or with no protein introduced prior to antiH5N1) steadily increased due to the specific binding of antiH5N1 until a steady-state surface coverage of the aptamer/H5N1/antibody assay complex was achieved. This data indicates that the antibody and aptamer probes bind to different epitopes on the protein target.

3.3. Quantitative analysis of H5N1

Accepted manuscript

Prior to applying the electrochemical sensing strategy to real sample analysis, the electrocatalytic reaction of the formed aptamer/H5N1/antiH5N1-ALP complex with APP was characterized using both cyclic (CV) and differential pulse voltammetry (DPV). A series of CV measurements are shown in figure 3(a) where the H5N1 concentration was varied while utilizing fixed concentrations of 50 nM antiH5N1-ALP and 60 µM APP. The same antibody and enzyme substrate concentrations were used for all the experiments reported here. The choice of 60 µM APP is based on previous work by us (Nam et al., 2012) while a series of preliminary measurements (shown in fig. S1) were performed to establish the optimum concentrations of 10 nM for the surface immobilization of the aptamer probe and also 50 nM for the antiH5N1-ALP concentration exposed to the chip surface. These concentrations were subsequently used for all further experiments.

The cyclic voltammetry measurements in figure 3a compares the current detection response as the H5N1 concentration is varied from 1 pM to 100 pM. In the absence of APP, no distinctive voltammetric peak was obtained. When the APP substrate was in contact with the aptamer/H5N1/antiH5N1-ALP sandwich complex, an oxidation peak appeared on a forward scan at around -0.05 mV vs. Ag/AgCl due to the reaction of ALP and APP. The increase in oxidation peak current as a function of H5N1 concentration

Accepted manuscript

also indicates the intact bioactivity of the aptamer attached on the electrode surface. A detectable concentration of 1 pM H5N1 with a sensitivity of 0.034 $\mu A\, pM^{-1}$ was achieved via cyclic voltammetry.

The sensitivity of the biosensor for H5N1 detection was further enhanced using the DPV technique. A series of differential pulse voltammograms for different H5N1 concentrations ranging from 100 fM to 100 pM in 50 mM Tris buffer (pH 8.5) are displayed in figure 3b where a step potential, pulse interval and amplitude of 20 mV/s, 50 ms and 50 mV, respectively, were employed throughout. The sweep direction was from a negative to a positive potential with an oxidation peak again observed at -0.05 mV in the presence of both the surface complex and APP and also increased with respect to H5N1 concentration. Each data point represents the average signal of five separate biosensors and the chip to chip variation was found to be within 10% indicating good reproducibility; this variation in the measurements may originate from differences in the overall surface coverage of gold nanoparticles deposited by chronoamperometry.

A summary comparison between the CV and DPV measurements is shown in figure 4 where the protein target concentration is the only variable besides the electrochemical technique used. At lower concentrations (100 fM to 10 pM) both techniques respond

Accepted manuscript

linearly with the DPV sensitivity (0.062 $\mu A\,pM^{-1}$, plot B) about two times higher than that from the CV measurements (plot A). At higher concentrations from 25 pM to 100 pM (plot C), a sensitivity of 0.01 $\mu A\,pM^{-1}$ (DPV data) was observed which is much lower than that obtained at low pM concentrations. The observation of two different linear response ranges is commonly observed on surface based bioaffinity sensors (e.g. (Karim and Lee, 2013; Karim et al., 2014; Nasirizadeh et al., 2013; Lee et al., 2014), with different sensitivities at lower and higher surface coverages. In our case this occurs at target concentrations below and above ~10 pM. Furthermore, at target concentrations higher than 100 pM, the sensor response becomes saturated (Thu et al., 2013; Hassen et al., 2008).

Possible non-specific contributions to the detection signal were also investigated prior to applying the biosensors to real sample analysis. This issue is always a concern when performing surface bioaffinity sensing (Li et al., 2011; Wang et al., 2009; Lin et al., 2015). Four different negative control sets were designed to demonstrate false positive signals due to non-specific interactions on the aptamer modified electrode (see Table 1). NC1 is antiH5N1-ALP adsorbed onto the aptamer surface in the absence of H5N1 protein; NC2 is for BNP protein instead of H5N1 adsorbed onto the aptamer surface followed by the non-specific adsorption of antiH5N1-ALP; NC3 is when the

Accepted manuscript

aptamer/H5N1 complex is exposed to antiAAT-ALP instead of antiH5N1-ALP; NC4 is for the sequential binding of H5N1 and antiH5N1-ALP onto a control aptamer sequence instead of the H5N1 aptamer.

Figure 5 shows a series of DPV measurements comparing the NC1-NC4 control responses versus the detection signal at a target concentration of 100 fM. All four negative control sets show electro-oxidative currents of ~0.5 µA at -0.05 mV due to the non-specific adsorption of ALP conjugates onto the electrode surface. When comparing the data for the NC controls versus 100 fM detection the lower responses (i.e. 0.5 µA vs 1 µA) and the different shapes of the NC current peaks demonstrates that the 100 fM detection signal for the H5N1 assay is clearly distinguishable from non-specific background contributions. The lowest detectable concentration of 100 fM H5N1 established here is significantly better than that of other nanoparticle modified electrochemical sensors recently reported for viral protein, 1.4 µM (Kamikawa et al., 2010) and H5N1 gene detection 0.43 pM (Kamikawa et al., 2010; Liu et al., 2011), and some DNA sensors based on fluorescence (0.3 nM, Cai et al., 2012) and transistor (1.25 pM, Thu et al., 2013) based detection. Furthermore, the 100 fM detection limit of the aptamer-antibody sandwich platform compares favorably with commercial antibody

Accepted manuscript

ELISA kits (e.g. www.novateinbio.com; www.creative-diagnostics.com; www.sinobiological.com)

An additional series of control measurements were performed to demonstrate the selectivity of the H5N1 detection measurement in the presence of an excess of common interfering serum proteins (Pang et al., 2015). This is described in the supporting information (see fig. S2) for (a) human serum albumin (HSA) and (b) immunoglobulin G (IgG). In each case, DPV measurements were compared for 500 fM H5N1 detection both separately and in the presence of a 100-fold excess concentration of each serum protein species. The results show that at 50 pM serum protein concentrations the background signal is about 8% increased with respect to the H5N1 in buffer only measurement, indicating there is a small non-specific contribution from albumin and IgG. Using the approach developed by (Macca and Wang, 1995) for evaluating the selectivity of amperometric sensors, selectivity coefficients ($\log k_{i,j}^{amp}$) of -3.34 and -3.04 were obtained for HSA and IgG (see fig. S2), respectively which indicate good selectivity towards the H5N1 target. However, the 50 pM serum protein concentrations used here are still considerably lower than the ca. millimolar concentrations of albumin typically found in undiluted serum.

Accepted manuscript

ACCEPTED MANUSCRIPT

3.4. Application of H5N1 sensors in diluted serum samples

As a demonstration, our sensor was next applied to the detection of H5N1 in real biological fluids, such as serum samples. Since the serum sample contained no H5N1, we attempted to spike various concentrations of H5N1 into differently diluted serum solutions and co-relate the current response due to the H5N1 present in serum solution to the added known concentration of H5N1 in buffer conditions. At least 100x dilution of serum samples was necessary due to the rise in the background current at a potential of around -0.05 mV vs. Ag/AgCl. The relative background contribution of albumin to the detection signal is described later in this section.

Figure 6a shows a series of DPV responses for 100 times diluted serum and also the diluted serum solutions spiked with H5N1 concentrations ranging from 500 fM to 10 pM. As the known concentration of H5N1 added was increased, the peak current at -0.05 mV due to the reaction of APP and the aptamer/H5N1/antiH5N1-ALP assay also increased with a measured slope of 0.063 $\mu A\, pM^{-1}$ (see fig 6b). Similar repeat measurements were performed in different serum dilutions ranging from 500 to 5000 times, with H5N1 concentrations ranging from 500 fM to 10 pM added to each dilution (see Fig S3). The DPV peak responses from all measurements with respect to the spiked known H5N1 concentrations are also compared in figure 6b revealing slopes of 0.067, 0.062, 0.082,

Accepted manuscript

0.057 μA pM^{-1} for 500, 1000, 2500 and 5000x diluted serum samples, respectively, all of which are fairly close to that of 100 times diluted serum (see also Table S1). In addition, the slope values obtained in diluted serum are a close match to the sensitivity of 0.062 μA pM^{-1} obtained for the same H5N1 concentration range of 100 fM to 10 pM in buffer medium. This indicates that our sensor can be employed for the quantitative analysis of H5N1 in biological fluids.

The small variation observed in sensitivity along with a low background current signal of ~0.4 μA at around -0.05 mV in fig. 6a are attributed to matrix effects, which may come from the non-specific adsorption of serum proteins such as albumin, which is the most abundant serum protein (Masaki et al., 2006; Fasano et al., 2005), alongside antiH5N1-ALP onto the aptamer surface. This was verified by investigating the response from our aptamer sensors exposed to different concentrations of albumin and antiH5N1-ALP followed by the interaction of APP (see fig S4). In order to make the albumin concentration similar to the albumin present in differently diluted serum samples (Fasano et al., 2005), albumin concentrations ranging from 140 nM to 1.4 μM were used. As the albumin concentration was increased, the peak current at the potential ranging from -0.02 mV to 0.09 mV increased. Interestingly, the DPV peak potential varied independently of albumin concentrations ranging from 140 nM to 1.4 μM which indicates that nonspecific

Accepted manuscript

behavior occurred randomly, but the peak value was still lower than for the detection of 500 fM of H5N1.

4. Conclusions

A portable biosensing platform was demonstrated for the sensitive and selective electrochemical detection of H5N1 viral proteins. This was based on the introduction of a new DNA aptamer/H5N1 protein/ALP labeled antiH5N1 sandwich complex on gold nanoparticle modified carbon electrodes. The introduction of a new aptamer and antibody pairing with each having different epitopes towards the H5N1 viral protein has advantages over conventional ELISA measurements through the use of an aptamer-functionalized surface (versus antibody) and improved sensitivity, specificity and selectivity. However, the preparation of the sensor chips is more involved than that of a typical ELISA multi-well platform but offers more control over non-specific adsorption. The lowest detectable concentration of 100 fM H5N1 reported is better than that of other electrochemical bioaffinity sensors (Kamikawa et al., 2010; Cai et al., 2012; Thu et al., 2013; Liu et al., 2011). This enhancement is possibly due to the advantages of associated with utilization of high affinity aptamers (compared to antibodies) for creating functionalized surfaces and the enlarged electroactive surface area due to the use of Au nanoparticles. Our sensors possess advantageous features including disposability and

Accepted manuscript

ACCEPTED MANUSCRIPT

easy field applicability and were also satisfactorily applied to the analysis of spiked H5N1 in human serum samples. Reproducibility was found to be RSD value of about 10 % and future work will be undertaken to improve upon this even further by achieving greater uniformity of the nanoparticle electrode deposition processes. We envision that the developed sensors can be effectively applied for the sensitive and selective sensing of avian influenza virus (H5N1) in biological specimens.

Acknowledgments

This research was supported by the Basic Science Research Program through the National Research Foundation of Korea (NRF) funded by the Ministry of Education, Science and Technology (NRF-2013R1A1A2A10005267) and also a National Research Foundation of Korea (NRF) grant funded by the Korea government (MSIP) (NRF-2013R1A2A2A03068833).

Accepted manuscript

References

Alonso-Lomillo, M.A., Yardimci, C., Domínguez-Renedo, O., Arcos-Martínez, M.J., 2009. Anal. Chim. Acta. 633, 51-56.

Alvarado-Gámez, A.L., Alonso-Lomillo, M.A., Domínguez-Renedo, O., Arcos-Martínez, M.J., 2015. Sensors 15, 2232-2243.

Barquero-Quirós, M., Domínguez-Renedo, O., Alonso-Lomillo, M.A., Arcos-Martínez, M.J., 2014. Sensors 14, 8203-8216.

Brockman, L., Wang, R., Lum, J., Li, Y., 2013. Open J. Appl. Biosens. 2, 97-103.

Burns, A., Mensbrugghe, D.v.d., Timmer, H., 2008. World Bank Report.

Cai, Q., Wang, C., Zhou, J., Luo, F., Lin, Z., Guo, L., Qiu, B., Chen, G., 2012. Anal. Methods 4, 3425-3428.

Cho, E.J., Lee, J.W., Ellington, A.D., 2009. Annu. Rev. Anal. Chem. 2, 241-264.

Desvaux, S., Garcia, J.M., Nguyen, T.D., Reid, S.A., Bui, N.A., Roger, F., Fenwick, S., Peiris, J.S.M., Ellis, T., 2012. Vet. Microbiol. 156, 277–284.

Dhumpa, R., Handberg, K.J., Jørgensen, P.H., Yi, S., Wolff, A., Bang, D.D., 2011. Diagn. Microbiol. Infect. Dis. 69, 258–265.

Dong, W., Luo, J., He, H., Jiang, L., 2013. Int. J. nanomed. 8, 221–232.

Fasano, M., Curry, S., Terreno, E., Galliano, M., Fanali, G., Narciso, P., Notari, S., Ascenzi, P., 2005. IUBMB Life 57, 787 – 796.

Guo, D., Zhuo, M., Zhang, X., Xu, C., Jiang, J., Gao, F., Wan, Q., Lia, Q., Wang, T., 2013. Anal. Chim. Acta. 773, 83-88.

Hassen, W.M., Chaix, C., Abdelghani, A., Bessueille, F., Leonard, D., Jaffrezic-Renault, N., 2008. Sens. Actuators B 134, 755–760.

Hayat, A., Catanante, G., Marty, J.L., 2014. Sensors 14, 23439-23461.

He, F., Soejoedono, R.D., Murtini, S., Goutama, M., Kwang, J., 2010. BMC Microbiol. 10, 1-9.

Hu, H., Voss, J., Zhang, G., Buchy, P., Zuo, T., Wang, L., Wang, F., Zhou, F., Wang, G., Tsai, C., Calder, L., Gamblin, S.J., Zhang, L., Deubel, V., Zhou, B., Skehel, J.J., Zhou, P., 2012. J. Virol. 86, 2978 –2989.

Ionescu, R.E., Cosnier, S., Herrmann, S., Marks, R.S., 2007. Anal. Chem. 79, 8662–8668.

Jackson, D., Killip, M.J., Galloway, C.S., Russell, R.J., Randall, R.E., 2010. Virology 396, 94–105.

Jang, H.R., Wark, A.W., Baek, S.H., Chung, B.H., Lee, H.J., 2014. Anal. Chem. 86, 814.

Kamikawa, T.L., Mikolajczyk, M.G., Kennedy, M., Zhang, P., Wang, W., Scott, D.E., Alocilja, E.C., 2010. Biosens. Bioelectron. 26, 1346-1352.

Karim, M.N., Lee, H.J., 2013. Talanta 116, 991-996.

Karim, M.N., Lee, J.E., Lee, H.J., 2014. Biosens. Bioelectron. 61, 147–151.

Lebarbenchon, C., Brown, J.D., Luttrell, M.P., Stallknecht, D.E., 2012. J. Vet. Diagn. Investig. 24, 161–165.

Lee, H.J., Wark, A.W., Corn, R.M., 2008. Analyst 133, 975–983.

Lee, S.H., Sumranjit, J., Tongkate, P., Chung, B.H., Lee, H.J., 2014. Electrochim. Acta. 123, 198–204.

Li, D., Wang, J., Wang, R., Li, Y., Abi-Ghanem, D., Berghman, L., Hargis, B., Lu, H., 2011. Biosens. Bioelectron. 26, 4146-4154.

Accepted manuscript

Limbut, W., Kanatharana, P., Mattiasson, B., Asawatreratanakul, P., Thavarungkul, P., 2006. Biosens. Bioelectron. 22, 233-240.

Lin, J., Wang, R., Jiao, P., Li, Y., Li, Y., Liao, M., Yu, Y., Wang, M., 2015. Biosens. Bioelectron. 67, 546-552.

Liu, X., Cheng, Z., Fan, H., Ai, S., Han, R., 2011. Electrochim. Acta. 56, 6266-6270.

Lum, J., Wang, R., Lassiter, K., Srinivasan, B., Abi-Ghanem, D., Berghman, L., Hargis, B., Tung, S., Lu, H., Li, Y., 2012. Biosens. Bioelectron. 38, 67-73.

Lv, M., Wei, M., Rong, F., Terashima, C., Fujishima, A., Gu, Z.-Z., 2010 Electroanalysis 22, 199–203.

Macca, C., Wang, J., 1995. Anal. Chim. Acta. 303, 265-274.

Masaki, T., Matsuura, T., Ohkawa, K., Miyamura, T., Okazaki, I., Watanabe, T., Suzuki, T., 2006. Biochem. J. 397, 345-353.

Moreno, A., Lelli, D., Brocchi, E., Sozzi, E., Vinco, L.J., Grilli, G., Cordioli, P., 2013. J. Virol. Methods 187, 424–430.

Nam, E.J., Kim, E.J., Wark, A.W., Rho, S., Kim, H., Lee, H.J., 2012. Analyst 137, 2011-2016.

Nasirizadeh, N., Shekari, Z., Zare, H.R., Ardakani, S.A.Y., Ahmar, H., 2013. J. Braz. Chem. Soc. 24, 1846-1856.

Nguyen, T.H., Ung, T.D.T., Vu, T.H., Tran, T.K.C., Dong, V.Q., Dinh, D.K., Nguyen, Q.L., 2012. Adv. Nat. Sci.: Nanosci. Nanotechnol. 3, 035014.

Pang, Y., Rong, Z., Wang, J., Xiao, R., Wang, S., 2015. Biosens. Bioelectron. 66, 527-532.

Pingarron, J.M., Yanez-Sedeno, P., Gonzalez-Cortes, A., 2008. Electrochim. Acta. 53, 5848–5866.

Renedo, O.D., Martínez, M.J.A., 2007. Anal. Chim. Acta. 589, 255-260.

Ricci, F., Adornetto, G., Palleschi, G., 2012. Electrochem. Acta. 84, 74–83.

Shiratori, I., Akitomi, J., Boltz, D.A., Horii, K., Furuichi, M., Waga, I., 2014. Biochem. Biophys. Res. Commun. 443, 37–41.

Thu, V.V., Tam, P.D., Dung, P.T., 2013. Curr. Appl. Phys. 13, 1311-1315.

Uyeki, T.M., Nguyen, D.C., Rowe, T., Lu, X., Hu-Primmer, J., Huynh, L.P., Hang, N.L.K., Katz, J.M., 2012. PLoS One 7, e43948.

Wang, C., Yan, Q., Liu, H.-B., Zhou, X.-H., Xiao, S.-J., 2011. Langmuir 27, 12058–12068.

Wang, R., Wang, Y., Lassiter, K., Li, Y., Hargis, B., Tung, S., Berghman, L., Bottje, W., 2009. Talanta 79, 159–164.

Wei, X., Zheng, L., Luo, F., Lin, Z., Guo, L., Qiu, B., Chen, G., 2013. J. Mater. Chem. B 1, 1812-1817.

Accepted manuscript

WHO, 2014. Influenza at the human-animal interface. http://www.who.int/influenza/human_animal_interface/Influenza_Summary_IRA_HA_interface_October14.pdf.
Zhu, M., Gong, X., Hu, Y., Ou, W., Wan, Y., 2014. J. Transl. Med. 12, 2-10.
Zhu, X., Ai, S., Chen, Q., Yin, H., Xu, J., 2009. Electrochem. Commun. 11, 1543–1546.

Figures and Table

Table 1. Negative controls used for assessing non-specific adsorption onto the aptamer modified electrode.

Biomolecule Type	NC1	NC2	NC3	NC4
Aptamer	H5N1 Aptamer			Control Sequence
Protein	None	BNP	H5N1	H5N1
Antibody	AntiH5N1		AntiAAT	AntiH5N1
Scheme	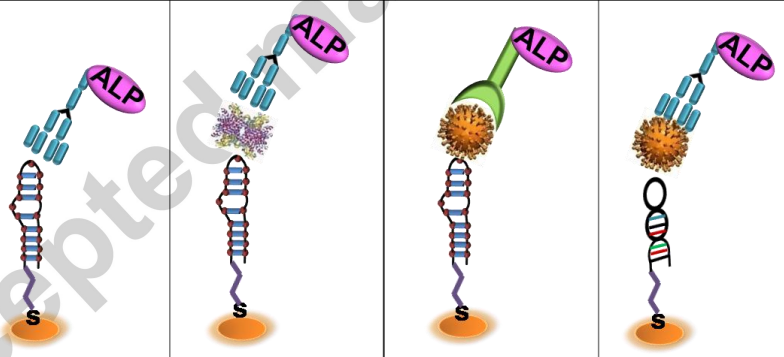			

Accepted manuscript

Figure 1. Schematic diagram of H5N1 viral protein detection using the enzymatic reaction of the substrate APP with the surface formed aptamer/H5N1/antiH5N1-ALP on a Au NP modified screen printed carbon electrode. A DNA aptamer probe specific to H5N1 was covalently immobilized onto the MPA functionalized Au NP's on the electrode surface through EDC/NHSS cross-linking chemistry. The specific adsorption of H5N1 protein and ALP tagged antiH5N1 onto the DNA aptamer surface was then detected via the APP redox reaction. All steps are described in the experimental section.

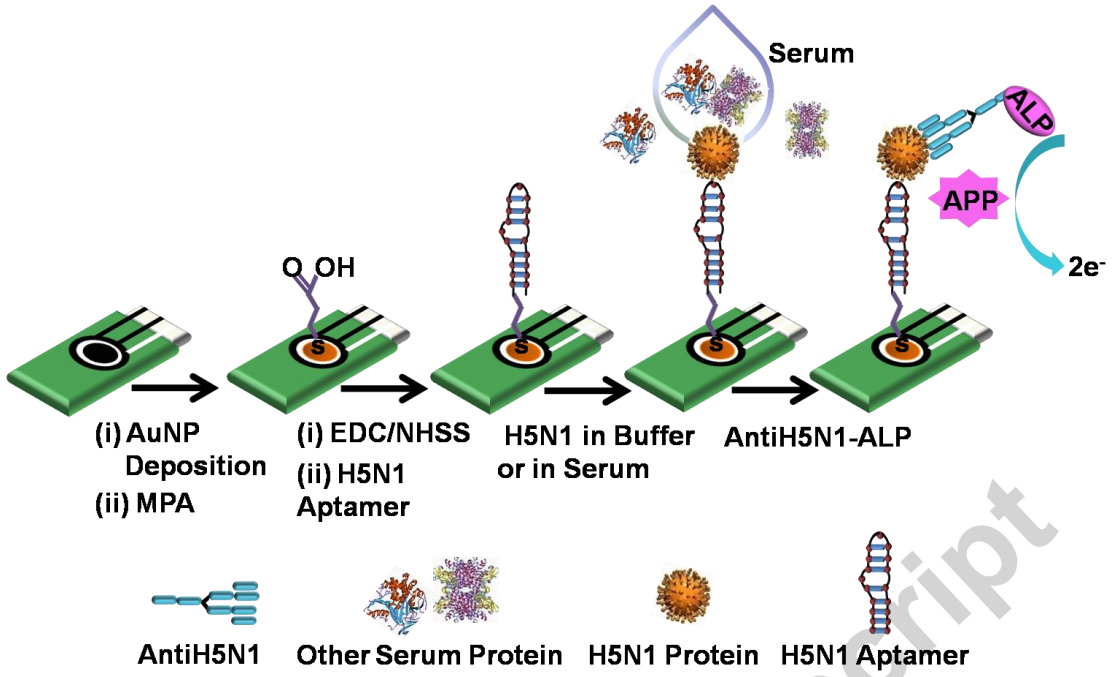

Figure 2. Langmuir isotherm plots of fractional surface coverage (θ) versus H5N1 concentration for the specific interaction (a) between H5N1 and surface immobilized antiH5N1, and (b) between H5N1 and surface bound DNA aptamer. (c) A plot of the normalized SPR response versus antiH5N1 concentration using an aptamer modified gold chip surface. The concentration of H5N1 in (c) was fixed as 200 nM and exposed to the chip prior to injecting buffer and then antiH5N1.

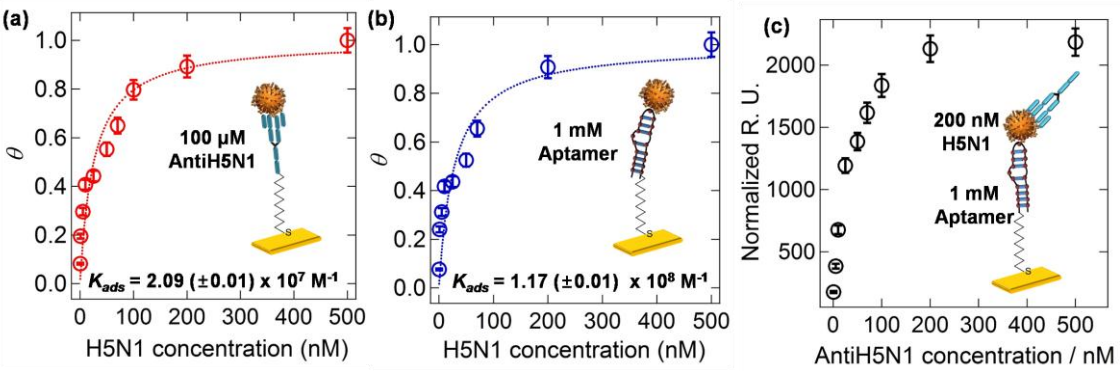

Figure 3. Representative (a) cyclic and (b) differential pulse voltammograms for the detection of H5N1 protein on DNA aptamer modified electrodes followed by the adsorption of antiH5N1-ALP and reaction with APP. The H5N1 concentration range was

from 1, 10, 50 to 100 pM in (a) and from 0.1, 5, 7.5, 25, 50 to 100 pM in (b). The APP concentration was fixed at 60 μM. The CV scan rate was 50 mV/s while for DPV measurements, a step potential of 20 mV/s, pulse interval of 50 ms and amplitude of 50 mV were used.

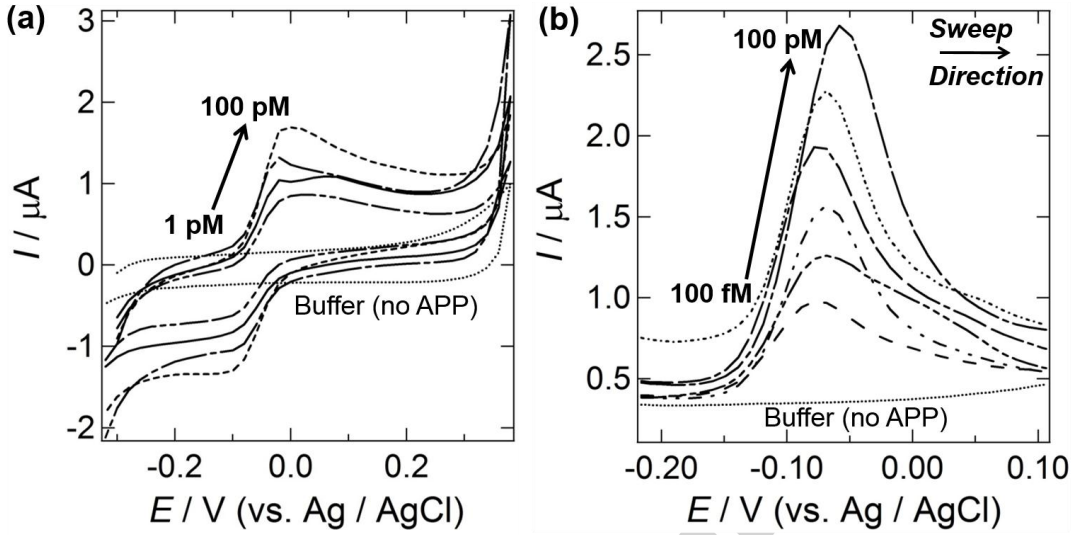

Figure 4. Comparison of peak current responses obtained for CV (A) and DPV (B), (C) measurements obtained over a range of H5N1 protein concentrations. In (A), the data points are from CV peak currents on the forward scan at H5N1 concentrations from 100 fM to 10 pM. In (B) and (C), DPV peak currents are plotted at H5N1 concentrations ranging from 100 fM to 10 pM and 25 pM to 100 pM, respectively. Dotted lines represent a linear fit.

Accepted manuscript

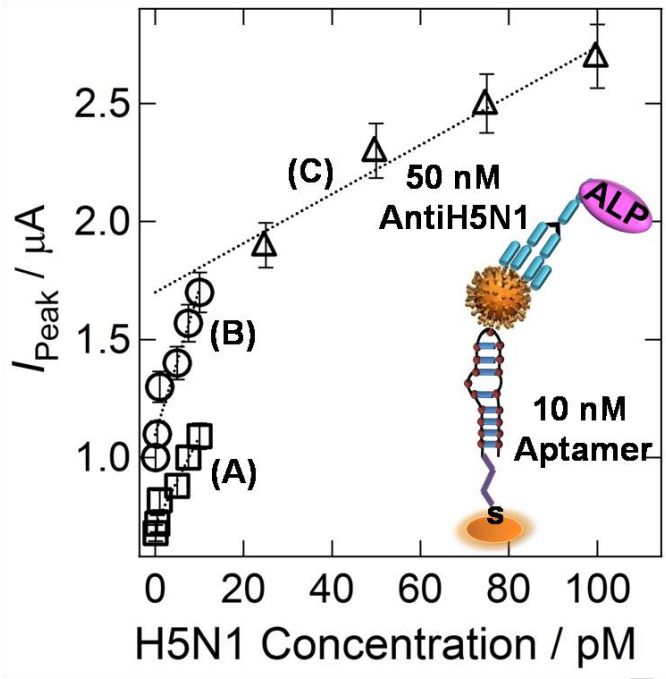

Figure 5. DPV measurements comparing 100 fM H5N1 detection to four different sets of negative control experiments. NC1 is in the absence of H5N1, NC2 is where 100 fM BNP is used instead of H5N1 protein, NC3 is 50 nM antiAAT-ALP used instead of antiH5N1-ALP, and NC4 is the replacement of the DNA aptamer with a control sequence. All other experimental parameters are the same as for Fig. 3b.

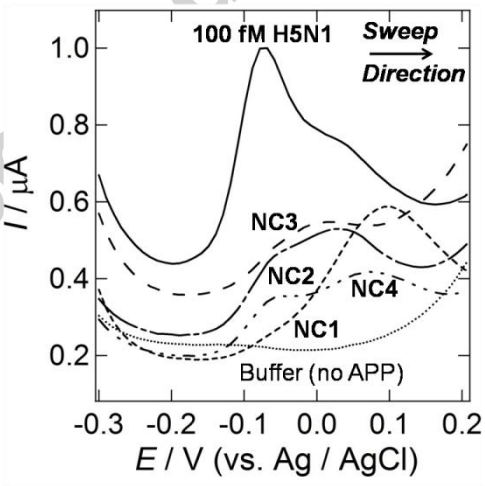

Accepted manuscript

Figure 6. (a) A series of differential pulse voltammograms for a 100x diluted human serum sample and following H5N1 spiking at 0.5, 1, 5, 7.5 and 10 pM. The experimental conditions for the DPV measurements were the same as in figure 3. (b) Plots of anodic peak current for the ALP-APP reaction product in differently diluted serum samples with varying H5N1 spiking concentrations. Dotted line represents the linear fit within the range of 0.5 to 10 pM. Serum samples were diluted 100, 500, 1000, 2500 and 5000 times in 10 mM PBS (pH 7.4) buffer.

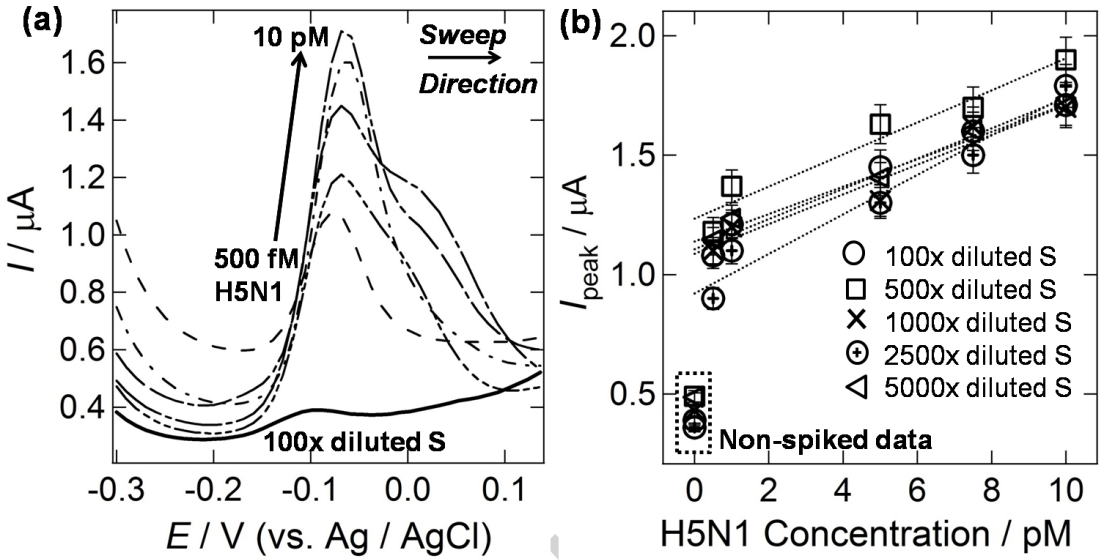

Graphical Abstract

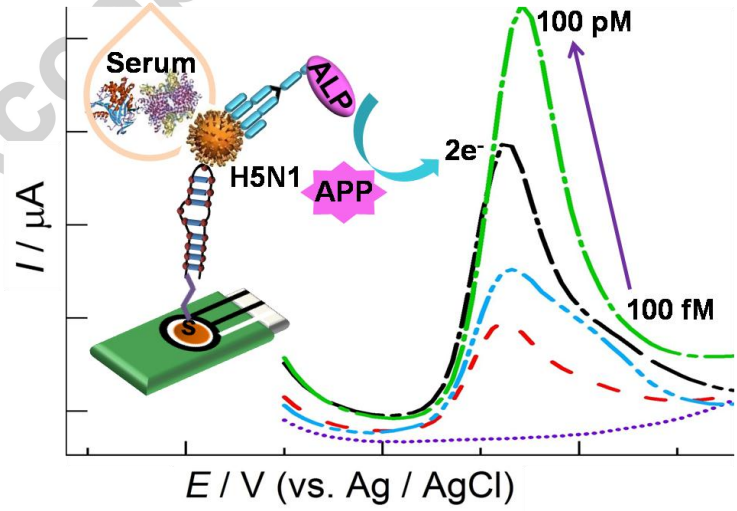

ACCEPTED MANUSCRIPT

Highlights:

- The introduction of a new aptamer-antibody sandwich assay pairing for the selective and sensitive detection of H5N1 viral protein. The strong binding affinity of each probe towards different epitope sites on H5N1 was confirmed.
- A new electrochemical biosensor utilizing the formation of a surface sandwich complex of DNA aptamer/H5N1 protein/antiH5N1-ALP.
- A lowest detectable concentration of 100 fM H5N1 protein with a linear dynamic range of 100 fM to 10 pM was demonstrated.
- The controlled electrodeposition of Au nanoparticles on a screen-printed carbon electrode (SPCE) provides a cost effective, convenient and reproducible sensing platform that can be potentially adapted to a wide range of biomolecular targets.
- Diluted human serum samples were directly analyzed for H5N1 viral proteins highlighting the potential of the platform for clinical diagnostic applications.

Accepted manuscript